Published in final edited form as:
Science. 2011 June 10; 332(6035): 1297–1300. doi:10.1126/science.1195639.

Endotoxin-Induced Structural Transformations in Liquid Crystalline Droplets

I-Hsin Lin[1], **Daniel S. Miller**[1], **Paul J. Bertics**[2], **Christopher J. Murphy**[3,4], **Juan J. de Pablo**[1], and **Nicholas L. Abbott**[1,*]

[1]Department of Chemical and Biological Engineering, University of Wisconsin–Madison, 1415 Engineering Drive, Madison, WI 53706–1607, USA

[2]Department of Biomolecular Chemistry, University of Wisconsin–Madison, 1300 University Avenue, Madison, WI 53706–1510, USA

[3]Department of Ophthalmology and Vision Science, School of Medicine, University of California, Davis, CA 95616, USA

[4]Department of Veterinary Surgical and Radiological Sciences, School of Veterinary Medicine, University of California, Davis, CA 95616, USA

Abstract

The ordering of liquid crystals (LCs) is known to be influenced by surfaces and contaminants. Here, we report that picogram per milliliter concentrations of endotoxin in water trigger ordering transitions in micrometer-size LC droplets. The ordering transitions, which occur at surface concentrations of endotoxin that are less than 10^{-5} Langmuir, are not due to adsorbate-induced changes in the interfacial energy of the LC. The sensitivity of the LC to endotoxin was measured to change by six orders of magnitude with the geometry of the LC (droplet versus slab), supporting the hypothesis that interactions of endotoxin with topological defects in the LC mediate the response of the droplets. The LC ordering transitions depend strongly on glycophospholipid structure and provide new designs for responsive soft matter.

The functional properties of inorganic and organic materials have been manipulated through the deliberate introduction of defects and grain boundaries, as well as through the partitioning of low concentrations of dopant species to these localized regions of the materials (1–4). For soft materials, such as liquid crystals (LCs), geometrical confinement within micrometer-sized systems has been shown to lead to the formation of a range of thermodynamically stable defects with nanoscopic dimensions and varied topologies (points, lines, rings) (5–11). In this paper, we report that confinement of LCs within micrometer-sized droplets dispersed in water can lead to ordering transitions in the LC droplets that are highly specific and sensitive to a particular bacterial glycophospholipid. These ordering transitions occur at concentrations of lipid that are six orders of magnitude lower than previously reported adsorbate-driven ordering transitions in LC systems (10–13).

Endotoxin is a bacterial lipopolysaccharide comprised of a glycophospholipid (called lipid A) (Fig. 1A) in addition to two polysaccharide domains. Lipid A has six tails, and thus it is

*To whom correspondence should be addressed: abbott@engr.wisc.edu.

Supporting Online Material
www.sciencemag.org/cgi/content/full/science.1195639/DC1
Materials and Methods
Figs. S1 to S4
References

structurally distinct from all other lipids (14). We investigated the interactions of endotoxin from *Escherichia coli*, the lipid A portion of endotoxin, and the other phospholipids and surfactants shown in Fig. 1, B to D, with micrometer-sized droplets of nematic LC [4′-pentyl-4-cyanobiphenyl (5CB)] (Fig. 1E) that were dispersed initially in endotoxin-free water (15). In the absence of endotoxin, bright-field (Fig. 1F) and polarized light micrographs (Fig. 1G) revealed the presence of two point defects (surface defects, called boojums) located at the "poles" of the LC droplets, corresponding to a so-called bipolar configuration of the droplet where the LC assumes a tangential orientation at the droplet surface (Fig. 1H) (5). After the addition of endotoxin to the water at a concentration of 1 μg/ml, both bright-field (Fig. 1I) and polarized light imaging (Fig. 1J) revealed a reordering of the LC within the droplet to a so-called radial configuration, corresponding to a single defect located at the droplet center and LC oriented perpendicular to the droplet surface (Fig. 1K) (5). Upon measuring the fraction of LC droplets within a solution of endotoxin that exhibited the radial configuration (Fig. 1L), we found that remarkably low concentrations of endotoxin (<1 pg/ml) trigger the ordering transition. Consistent with our conclusion that the interaction of the LC droplets and endotoxin was responsible for the ordering transition, the fraction of LC droplets in the radial configuration increased with the concentration of endotoxin (Fig. 1L). The response of the LC droplets to endotoxin was dependent on the total number of LC droplets in solution, allowing the ordering transition to be tuned over a range of endotoxin concentrations (e.g., 1 to 10 pg/ml or 1 to 100 pg/ml) (Fig. 1L). The lipid A portion of endotoxin caused similar ordering transitions in the LC droplets.

The simplest continuum description of the ordering of LCs within droplets considers the free energy, F, of each droplet to be influenced by an orientation-dependent surface free energy and an elastic strain free energy, namely $F \approx \int W dA + \frac{K}{2}\int (\nabla n)^2 dV$, where W is the so-called surface anchoring energy per unit area, A is the surface area of the droplet, K is the elastic modulus for strain of the LC (16), n is the director of the LC (16), and V is the volume of the LC droplet (5, 8, 10, 11). Past studies have demonstrated that lipids and synthetic surfactants can induce ordering transitions at aqueous-LC interfaces through a mechanism that involves an adsorbate-induced change in W (12, 13, 17). However, to change W to induce an ordering transition requires near saturation coverage of the interface by the adsorbate (0.1 to 1 Langmuir), typically corresponding to solution concentrations of lipids of at least ~10 μg/ml (10–13, 18). Consistent with a mechanism involving changes in W, we observed that double-tailed lipids such as 1,2-dilauroyl-*sn*-glycero-3-phosphatidylcholine (DLPC) and 1,2-dioleoyl-*sn*-glycero-3-phosphatidylcholine (DOPC) (Fig. 1, B and C) and single-tailed synthetic surfactants such as sodium dodecylsulfate (SDS) (Fig. 1D) induced ordering transitions in the LC droplets only at concentrations greater than 10 μg/ml (Fig. 2A). These results contrast to lipid A where ordering transitions are induced in the LC droplets at concentrations of lipid A that are at least six orders of magnitude lower (picograms per milliliter). We calculated that if all of the endotoxin in 40 μL of a 1 pg/ml solution adsorbed uniformly over the aqueous-LC interface of ~10^4 LC droplets (radius 3 μm) in one of our experiments (Fig. 1L), the interfacial density of endotoxin would be ~1 molecule/10^6 nm^2 or ~10^{-5} of saturation monolayer coverage (~10^{-5} Langmuir) (19). In contrast, the double-tailed lipids mentioned above (Fig. 1, B and C) trigger ordering transitions at interfacial concentrations that correspond to ~1 molecule/0.6 nm^2 (saturation coverage is ~1 molecule/0.4 nm^2). This pronounced difference in surface density of lipid (5 to 6 orders of magnitude) required to trigger ordering transitions within LC droplets led us to propose that, at pg/ml concentrations, endotoxin and lipid A do not trigger ordering transitions in the LC droplets through changes in W (as is the case for DLPC and DOPC) but instead trigger the ordering transitions through interaction with localized regions of the LC droplets. We hypothesized that the local regions of interaction were defined by the defects in the LC (Fig. 1, H and K).

Past studies have established that nematic LCs, when confined in certain geometries, cannot satisfy the boundary conditions of the system through continuous strain (splay, bend, and twist) of the LC (5, 7, 8, 10, 11). Instead, the LC satisfies the boundary conditions through the generation of nanoscopic regions within which the molecules comprising the LC possess low levels of orientational order, namely, defects such as the point defects shown in Fig. 1, H and K. We tested the role of defects in the LC ordering transitions induced by endotoxin and lipid A by changing the geometry of the LC system. First, we measured ordering transitions induced by spontaneous adsorption of endotoxin or lipid A at planar interfaces of LC that lack the defects generated by the spherical geometry of the droplets. At these planar interfaces, neither lipid A nor endotoxin triggered an ordering transition in the LC until the concentration exceeded ~1 μg/mL (fig. S1) (12, 15, 20, 21). Second, we formed Langmuir monolayers of lipid A of known density at the surface of water and transferred the lipid A monolayers onto planar aqueous-LC interfaces using the Langmuir-Schaefer transfer method (as illustrated in Fig. 2B) (13, 15). These measurements revealed that a surface concentration of lipid A of ~1 molecule/1.15 nm^2 was required to cause an ordering transition at the planar LC interface (Fig. 2C), a surface concentration that is six orders of magnitude greater than the surface concentration driving the ordering transition of the LC droplets. These observations, when combined with the results reported above, support our hypothesis that endotoxin and lipid A trigger ordering transitions in micrometer-sized LC droplets through interaction with defects in the LC that are induced by the spherical geometry of the LC droplets.

To provide further insight into the interaction of endotoxin with the defects of the LC droplets, we performed confocal fluorescence microscopy using boron dipyrromethene (BODIPY)–labeled endotoxin (Fig. 3A) (15). These measurements confirmed that endotoxin was localized at the point defect formed at the center of each LC droplet with a radial configuration. Interestingly, after deliberate photobleaching of the BODIPY-labeled endotoxin at the point defect, we measured a time-dependent recovery of the fluorescence (Fig. 3B), indicating an exchange of lipid between the center and surface of the droplet that occurred over tens of seconds. We also heated an emulsion of 5CB free of endotoxin above the clearing temperature of the nematic phase (T_{iso} = 35°C; experiments were performed at 50°C), added 10 pg/mL of endotoxin, and then cooled the sample through the isotropic-to-nematic phase transition. We measured the characteristic time interval between the formation of the nematic phase during cooling and the establishment of radial ordering (Fig. 3C) (22, 23). The time interval was found to scale with the square of the droplet radius, consistent with a physical process underlying the ordering transition that involved diffusion of the lipid. We calculated the time for diffusion of lipid across the surface of the LC droplet (calculated as $t_1 = L_A^2/4D_s$, where L_A corresponds to $\pi R/2$, the distance along the surface from the equator to the pole) to be in good agreement with the data in Fig. 3C [using $D_s \sim 10 \times 10^{-12}$ m^2/s (12)]. The surface diffusion time for a droplet with a radius of 3 μm was calculated to be ~0.6 s; the experimentally measured characteristic time was ~1 s (Fig. 3C) (22, 23). This result suggests a physical process in which the dynamics of the ordering transition induced by endotoxin are governed by the lateral transport of endotoxin across the surface of the LC droplet, a process that would be necessary to localize endotoxin at surface defects (boojums) to initiate the ordering transition. We note that past studies have reported observations of the localization of inorganic colloids at defects generated in LC systems (24, 25), including stabilization of blue phases (26). We also observed 10 pg/ml of endotoxin to trigger the ordering transition from the bipolar to the radial configuration through a kinetic pathway that was distinct from that observed during the surface-driven ordering transitions caused by DLPC, SDS, lecithins and concentrations of endotoxin (50 μg/ml) that were sufficient to saturate the LC interface (10, 11, 27). The distinct kinetic pathway triggered by 10 pg/ml of endotoxin provides further support for our conclusion that the ordering

transitions at low concentrations of endotoxin are not caused by changes in surface anchoring energy (W).

In summary, our experiments establish that the effect of endotoxin at concentrations of ~1 pg/ml on the surface anchoring energy of LCs is negligible; ordering transitions in LC droplets driven by changes in surface anchoring energy require six orders of magnitude higher surface concentrations of lipid than are present in our experiments with endotoxin. Furthermore, we do not expect the endotoxin to change the elastic moduli of the LC and thus drive the ordering transition through a lowering of the elastic energy. Instead, the experimental results reported in this paper are consistent with the proposition that the ordering transitions in micrometer-sized LC droplets are driven by the interactions of endotoxin with topological defects induced by the geometry of the LC droplets. Our observation that the ordering transitions of the LC droplets are specific to the lipid structure of endotoxin suggests that endotoxin may be forming organized assemblies within the cores of the defects to change the defect energies to favor stabilization of the radial configuration over the bipolar structure. In comparison with previously reported ordering transitions involving planar LC films, we find that endotoxin-driven ordering transitions in LC droplets are ~10^6 times more sensitive. This sensitivity and structure-based selectivity of ordering transitions in LC droplets suggests new principles for the design of responsive LC systems, particularly for the design of sensors that respond to targeted biological analytes (28, 29).

Supplementary Material

Refer to Web version on PubMed Central for supplementary material.

Acknowledgments

This work was primarily supported by NSF through DMR-0520527 (Materials Research Science and Engineering Center), the Army Research Office (W911NF-07-1-0446 and W911NF-06-1-0314), and the National Institutes of Health (CA108467 and CA105730). The technical assistance of B. Carlton is gratefully acknowledged. A patent application based on this work has been filed by the Wisconsin Alumni Research Foundation (P09241US02). N.L.A. and C.J.M. are members of the board of directors of Platypus Technologies LLC, a startup company set up to develop analytic methods based on liquid crystals.

References and Notes

1. Hu D, et al. Nature. 2000; 405:1030. [PubMed: 10890438]
2. Queisser HJ, Haller EE. Science. 1998; 281:945. [PubMed: 9703502]
3. Romalis M. Nature. 2008; 455:606. [PubMed: 18833268]
4. Simon J, Protasenko V, Lian CX, Xing HL, Jena D. Science. 2010; 327:60. [PubMed: 20044569]
5. Lavrentovich OD. Liquid Crystals. 1998; 24:117.
6. Lee BW, Clark NA. Science. 2001; 291:2576. [PubMed: 11283364]
7. Musevic I, Skarabot M, Tkalec U, Ravnik M, Zumer S. Science. 2006; 313:954. [PubMed: 16917058]
8. Poulin P, Stark H, Lubensky TC, Weitz DA. Science. 1997; 275:1770. [PubMed: 9065396]
9. Zapotocky M, Ramos L, Poulin P, Lubensky TC, Weitz DA. Science. 1999; 283:209. [PubMed: 9880250]
10. Prischepa OO, Shabanov AV, Zyryanov VY. JETP Lett. 2004; 79:257.
11. Volovik GE, Lavrentovich OD. Sov Phys JETP. 1983; 58:1159.
12. Brake JM, Daschner MK, Luk YY, Abbott NL. Science. 2003; 302:2094. [PubMed: 14684814]
13. Meli MV, Lin IH, Abbott NL. J Am Chem Soc. 2008; 130:4326. [PubMed: 18335929]
14. Raetz CRH, Whitfield C. Annu Rev Biochem. 2002; 71:635. [PubMed: 12045108]
15. Materials and methods are available as supporting material on *Science* Online.

16. This simple model assumes the elastic modulus for splay, bend, and twist of the LC to be equal in magnitude. The director is a vector that is used to describe the average orientation of molecules within an LC.
17. Gupta JK, Sivakumar S, Caruso F, Abbott NL. Angew Chem Int Ed. 2009; 48:1652.
18. Sivakumar S, Wark KL, Gupta JK, Abbott NL, Caruso F. Adv Funct Mater. 2009; 19:2260.
19. Assumptions underlying the calculation: (i) the molecular weight of endotoxin is 50 kD, (ii) the emulsion droplets have radii of 3 μm, and (iii) endotoxin in solution adsorbs uniformly over the interface of all LC droplets.
20. McCamley MK, Artenstein AW, Opal SM, Crawford GP. Proc SPIE. 2007; 6441:64411Y.
21. McCamley MK, et al. J Appl Phys. 2009; 105:123504.
22. For LC droplets with diameters smaller than 10 μm, the kinetics of formation of the nematic phase are fast (<50 ms) compared with the dynamics of the transformation leading to the appearance of the radial configuration of the nematic phase.
23. Chen XC, Hamlington BD, Shen AQ. Langmuir. 2008; 24:541. [PubMed: 18081328]
24. Fernández-Nieves A, et al. Phys Rev Lett. 2007; 99:157801. [PubMed: 17995213]
25. Skarabot M, et al. Phys Rev E Stat Nonlin Soft Matter Phys. 2008; 77:031705. [PubMed: 18517404]
26. Ravnik M, Alexander GP, Yeomans JM, Zumer S. Faraday Discuss. 2010; 144:159. 467. discussion 203. [PubMed: 20158028]
27. The kinetic pathway of the transition between the bipolar and radial configurational states of the LC droplets was characterized by videomicroscopy (see figs. S2 to S4).
28. Endotoxin is an indicator of bacterial contamination. Detection of endotoxin in purified water (in the 1 to 100 pg/ml range) is widely performed during manufacturing processes for pharmaceutical products (including validation of water used in such processes) and biomedical devices, in a variety of public health contexts (particularly analysis of aerosols in industrial and indoor environments) and for biological research.
29. Cohen J. Nature. 2002; 420:885. [PubMed: 12490963]

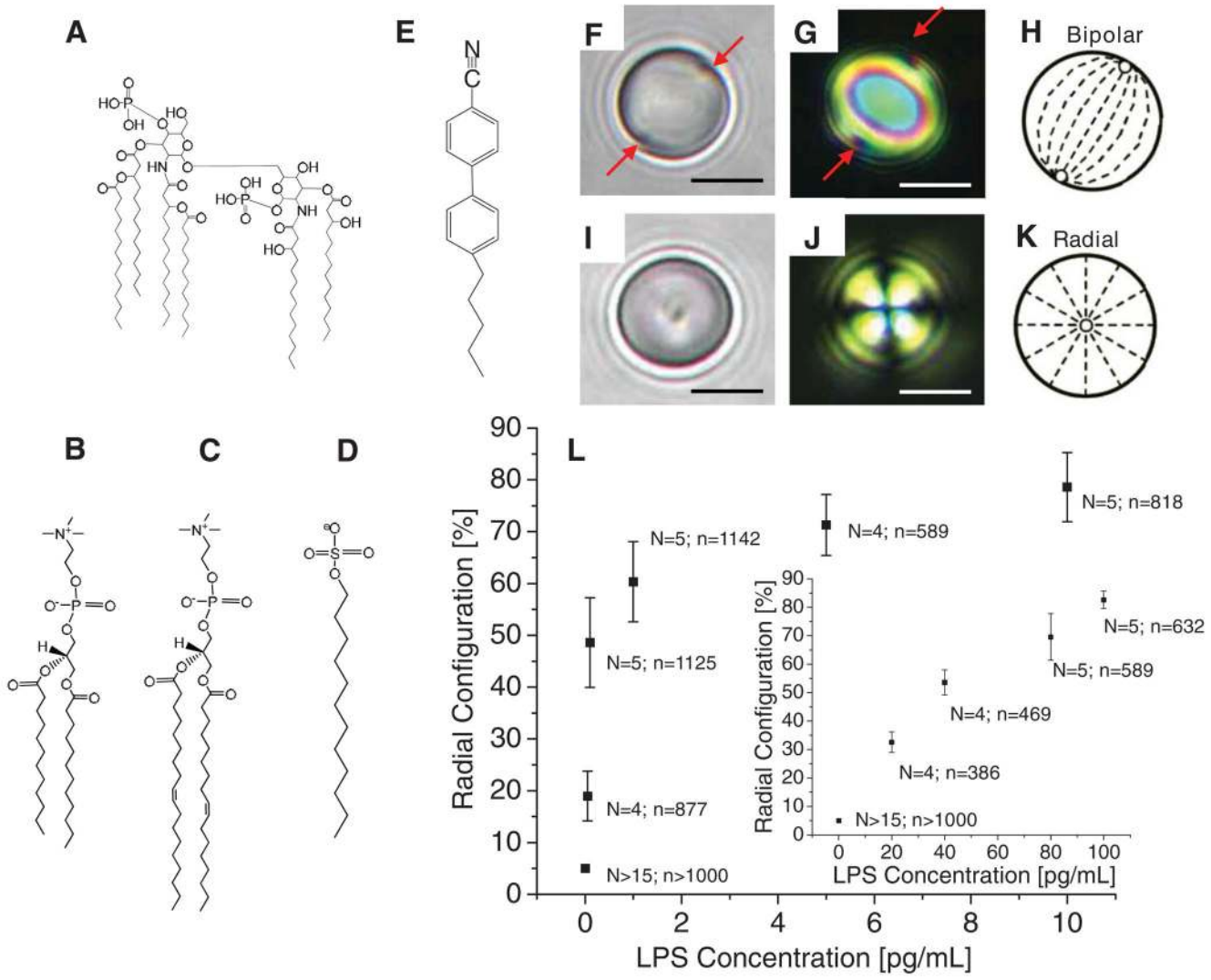

Fig. 1.

(**A**) Lipid A portion of endotoxin. (**B**) DLPC. (**C**) DOPC. (**D**) SDS. (**E**) 5CB. (**F** and **G**) Bright-field (F) and polarized light (G, crossed-polars) micrographs of an LC droplet in endotoxin-free water (15). The red arrows indicate boojums at the aqueous-LC interface of the droplet. (**H**) Schematic illustration of the bipolar configuration of the LC droplet corresponding to (F) and (G). (**I** and **J**) Bright-field (I) and polarized light (J, crossed-polars) micrographs of an LC droplet after exposure to endotoxin from *E. coli* (O127:B8; 1 μg/mL) in water. (**K**) Schematic illustration of the radial configuration of the LC droplet corresponding to (I) and (J). (**L**) Percentage of 8300 LC droplets in 40 μL of water that exhibited a radial configuration, plotted as a function of endotoxin concentration. The inset shows the response of the LC droplets when 94,000 droplets were used. The LC-in-water emulsion droplets (diameters of ~4 to 8 μm) were prepared by sonication of nematic 5CB in water that was free of endotoxin (15). The droplet numbers were determined using flow cytometry (15). Endotoxin concentrations were validated using an independently experiments, and *n* indicates the total number of LC emulsion droplets that were analyzed. Scale bars, 5 μm.

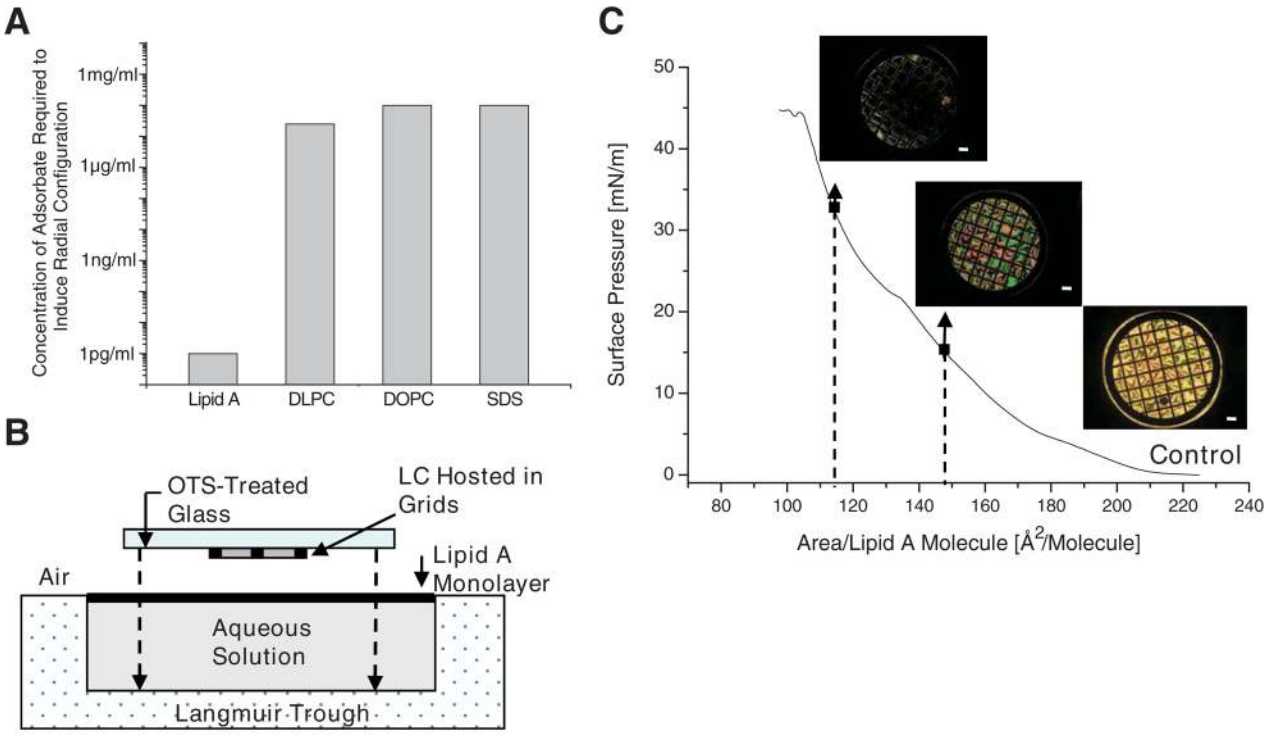

Fig. 2.

(**A**) Bulk concentrations of lipids or surfactants in solution (40 μL) required to cause at least 50% of 8300 LC droplets added to each solution to adopt a radial configuration. (**B**) Schematic illustration of the experimental apparatus used to transfer Langmuir monolayers of lipid A at prescribed surface densities from an air-water interface onto a planar aqueous-LC interface (13). In brief, micrometer-thick films of nematic 5CB (with planar interfaces) were prepared within the pores of Au grids supported on glass slides treated with octadecyltrichlorosilane (to cause perpendicular ordering of the LC). The supported LC was then immersed downward through the lipid A monolayer at the surface of the water (15) to transfer the monolayer onto the planar aqueous-LC interface. (**C**) Surface pressure-area isotherm measured for a Langmuir monolayer of lipid A and the optical appearance (between crossed polars) of films of 5CB with planar interfaces (hosted within the metallic grids) after transfer of Langmuir films of lipid A at the indicated interfacial density onto the 5CB-aqueous interface [see (B) for details]. The control corresponds to LC passed into endotoxin-free water. The bright optical appearance of the control indicates an orientation of the LC that is parallel to the aqueous-LC interface. The optical appearance of the sample prepared at an area per molecule of lipid A of 148 $Å^2$/molecule indicates a tilted state of the LC. The dark optical appearance of the sample prepared at 115 $Å^2$/molecule indicates a perpendicular orientation of the LC at the aqueous interface. Scale bars, 300 μm.

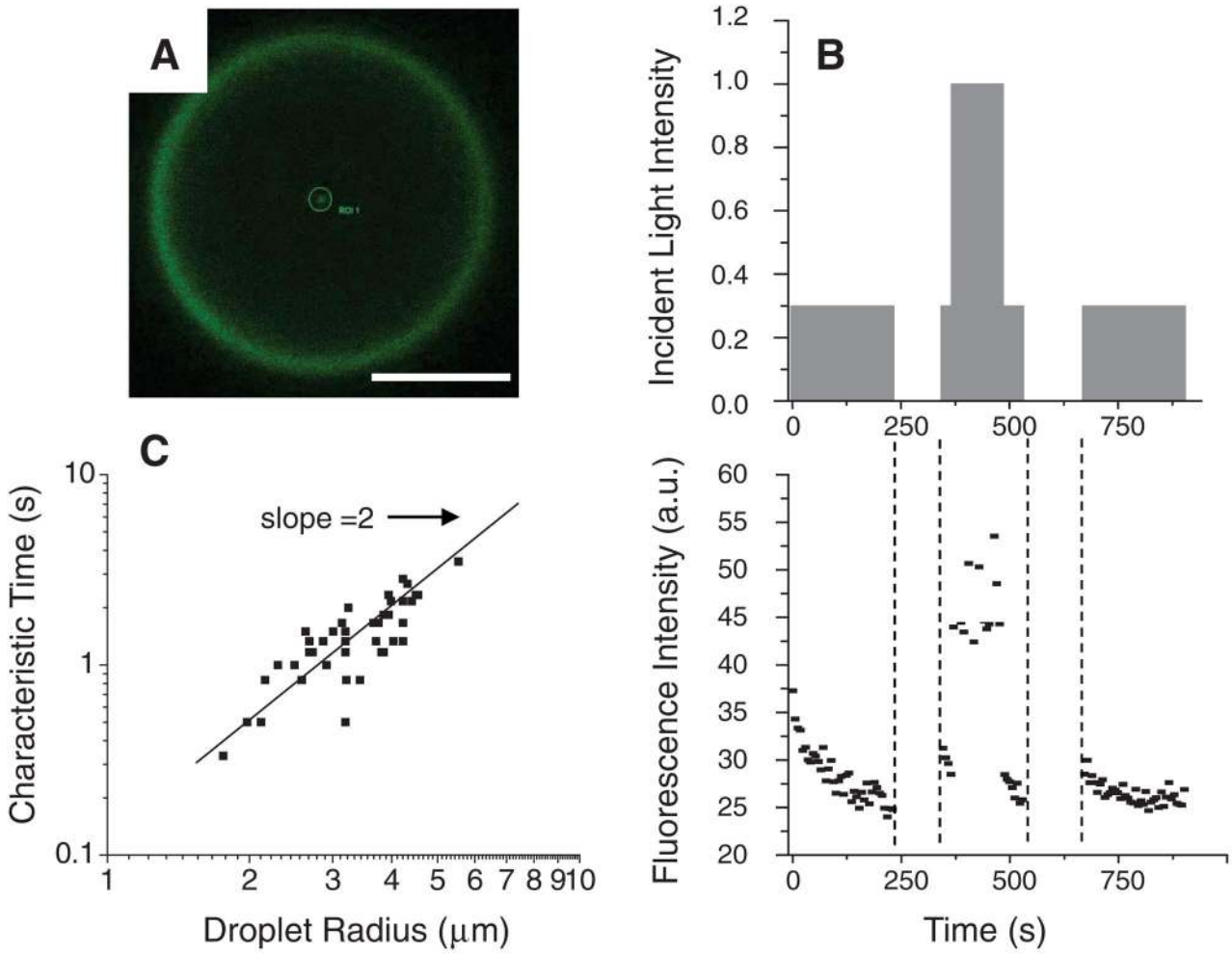

Fig. 3.

(**A**) Confocal fluorescent micrograph of an LC droplet in contact with a solution of BODIPY-labeled endotoxin. The point defect at the center of the droplet with a radial configuration exhibits a strong fluorescence signal. The concentration of endotoxin in solution was 20 μg/ml in order to achieve a sufficient signal intensity to image the droplets. Imaging was performed using an argon laser at an excitation wavelength of 488, and the detector collected the emission with wavelengths from 499 nm to 634 nm (15). Scale bar, 5 μm. (**B**) Photobleaching of the BODIPY-labeled endotoxin at the center of the LC droplet. The upper panel shows the intensity of the excitation laser, and the lower panel shows the corresponding fluorescence intensity. Loss of fluorescence signal is apparent during the periods of sample illumination (e.g., 0 to 230 s), and recovery of fluorescence is apparent in the periods of time when the laser incident on the sample was blocked (e.g., 230 to 350 s); A.U. indicates arbitrary units. The incident light intensity is indicated as a fraction of the maximum laser power. (**C**) Time taken for LC droplets to exhibit radial ordering after a thermal quench from the isotropic to nematic phase, plotted as a function of the droplet radius. The experiment was performed with 21,500 LC droplets dispersed in 100 μL of solution containing 10 pg/mL endotoxin. The line shown in the figure has a slope of 2.